

# Adsorption of charged macromolecules on oppositely charged porous column materials

Vesela Malinova, Ruth Freitag, Christine Wandrey\*

Swiss Federal Institute of Technology, Institute of Chemical and Biological Process Science,  
EPFL-ISP-LBCH, CH-1015 Lausanne, Switzerland

## Abstract

A family of cationic polyelectrolytes possessing defined chain lengths, narrow chain length distributions, uniform charge density, but substituents of different hydrophilicity at the quaternary ammonium group served as model compounds for adsorption studies. These studies quantitatively revealed that polymer characteristics and electrostatic parameters affect the adsorption behavior on oppositely charged porous column materials. The presence of electrostatic exclusion, in addition to size exclusion, was proved comparing molecular, electrostatic and geometrical parameters. The dominance of electrostatic effects could be concluded evaluating the relation between molecular and electrostatic dimensions. The results provide a contribution how to estimate the threshold for electrostatic exclusion from pores as a function of dimensions and experimental conditions.

© 2003 Elsevier B.V. All rights reserved.

*Keywords:* Adsorption; Adsorption isotherms; Electrostatic interactions; Polyelectrolytes; Polymers

## 1. Introduction

Interactions of charged macromolecules, polyelectrolytes, on oppositely charged surfaces and interfaces are a classical problem of physical chemistry and polymer physics. The broad interest in this problem is stimulated by its tremendous importance for many areas of the natural sciences ranging from material sciences to process sciences and life sciences. Advances in the understanding of this complicated topic have found their practical applications, for example, in bioengineering, colloid stabilization/destabilization or surface design. The majority of experimental studies, theoretical approaches and simulations relate, however, to the interaction of polymers with flat homogeneous surfaces. In comparison, data for the interaction/adsorption of charged macromolecules on oppositely charged curved surfaces including porous materials are rare. One can also make the same claim regarding physical chemical models. Therefore, at present, no comprehensive theoretical approach exists to link molecular parameters and system conditions with the porous materials characteristics. From the few existing results it is evident that size exclusion and/or electrostatic

exclusion are present and influence, in addition to the non-hindered adsorption process, the extent of the surface availability. Consequently, there is a need for appropriate studies using more sophisticated surfaces in association with model polyelectrolytes.

An accessible situation for such studies exists in chromatography where the molecules in question interact with a comparatively well-defined surface under controlled conditions. Specifically, ion exchange displacement chromatography serves two objectives. Firstly, the adjustable conditions of the displacement mode offer the opportunity to perform basic studies on the interaction of charged molecules with charged surfaces possessing various characteristics. Secondly, relationships from such basic studies can be used to optimize the chromatographic process for specific separation problems, to develop tailor-made displacers, and to predict optimum combinations of displacer and stationary phases.

Efficient separation and purification steps determine, to a large extent, the economy in biotechnology and pharmaceutical industry. In this context ion-exchange displacement chromatography has a high potential as preparative separation technique for biomolecules [1,2]. The resolving power of the displacement mode of chromatography has been demonstrated for challenging separation problems and has received considerable attention in the last years as an

\* Corresponding author. Tel.: +41-21-693-3672; fax: +41-21-693-6030.

E-mail address: [christine.wandrey@epfl.ch](mailto:christine.wandrey@epfl.ch) (C. Wandrey).

alternative to gradient chromatography for protein separation [3]. The optimization of displacement separation of macromolecules, on the other hand, poses a complex problem. Polyelectrolytes possessing a higher affinity are potential protein displacers. Several types of molecules have been screened, and tried, related to their performance as displacers for biomolecules [4–7]. However, the lack of relationships linking the chemical structure, the molecule size, and the performance of the displacer under process conditions complicate the process development. Some authors published the “chemical nature” as deciding parameter for the efficiency of the separation process without specifying this nature, for example, by precise physical parameters such as chain length, type of charge, charge density, and uniformity. Heterogeneity of a displacer concerning chain lengths and/or charge density will lead to band spreading and, probably, its dispersion within the protein peak [8].

In addition, there is a lack of understanding the effect of various stationary phase characteristics (chemistry, capacity, pore size, transport properties) on displacement separations. Stationary phase characteristics are expected to impact two aspects of displacement chromatography: the affinity of displacer molecules and the yield and production rates achievable with displacement separations [9].

On the other hand models, for example the steric mass action model, have been established which try to predict optimum conditions for displacement processes [10]. In general, the separation process of this type of chromatography is based on interactions of charged molecules with oppositely charged surfaces [11].

Electrostatic interactions of poly(vinylbenzylammonium chloride) (PVBAC) compounds in aqueous solutions, proposed in this paper as a model compound to study the adsorption on negatively charged porous surfaces, have been investigated and reported recently as a function of chain length, concentration, and chemical structure [12]. The availability of these basic data was the reason to select this type of positively charged macromolecules for the adsorption studies herein. Moreover, the synthesis route is relatively simple and offers the possibility to yield differently substituted molecules of the same degree of polymerization for which also the charge density can be modified [13,14]. As to the authors' knowledge this paper, for the first time, aims at quantifying the importance of electrostatic exclusion, in addition to size exclusion in chromatographic processes, where the separation is primarily based on electrostatic interactions, and it is intended to employ porous column materials.

## 2. Experimental

### 2.1. Materials

Differently substituted PVBAC samples have been used to monitor adsorption isotherms. Controlled radical

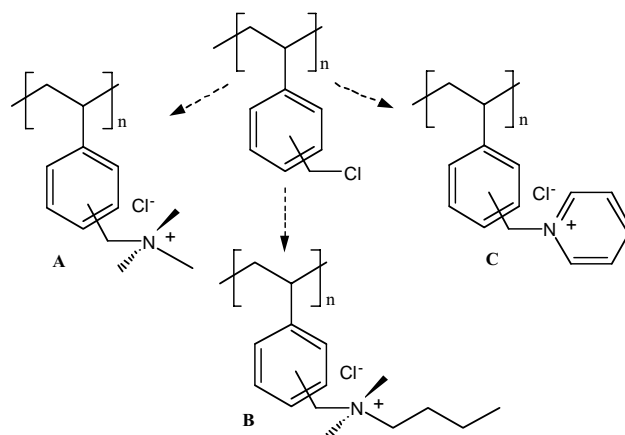


Fig. 1. Structures of the various poly(vinylbenzyltrialkylammonium chloride) model compounds synthesized from poly(vinylbenzyl chloride). (A) Trimethylammonium, (B) dimethyl-*n*-butylammonium, (C) pyridinium.

polymerization, previously described [13], has been applied for the synthesis of the narrowly distributed precursor poly(vinylbenzyl chloride) (PVBC) ( $M_w/M_n = 1.15$  for  $P_n = 25$  and  $M_w/M_n = 1.31$  for  $P_n = 90$ ). Reaction of PVBC with tertiary amines—trimethylamine, dimethyl-*n*-butyl, pyridine (Aldrich, Switzerland) results in cationic polyelectrolytes A, B, C (Fig. 1) with a charge distance of 0.25 nm and final molar masses of  $M_n = 5300, 5800, 6300$  g/mol for  $P_n = 25$  and 19 100, 21 000, 22 900 g/mol for  $P_n = 90$ .

Table 1 summarizes the molecular characteristics of all investigated samples.

Strong acidic cation-exchange (SAC) columns (MCX) were supplied by PSS (Mainz, Germany). Table 2 contains their dimensions and characteristics. NaCl (Fluka, Germany) was added to adjust the ionic strength.  $\text{NaNO}_3$ ,  $(\text{NH}_4)_2\text{SO}_4$ ,  $\text{KNO}_3$ , HCl (Fluka), NaOH (Merck, Germany) were used for the determination of the dead volume and ion capacity of the columns, respectively.

### 2.2. Polymer analysis and purification

Molar masses and polydispersity of the PVBC precursor were determined by size exclusion chromatography (SEC) column combination: poly(styrene-divinylbenzene) (PS-DVB)  $10^4, 10^3, 10^2$  (Knauer), 300 mm  $\times$  7.4 mm, eluent: tetrahydrofuran (THF), flow rate: 1 ml/min, standard: polystyrene. After quaternization the polymers were dialyzed against water [molecular mass cut-off (MWCO): 1000 and 6000] and freeze-dried. The degree of quaternization was determined recording  $^1\text{H}$  NMR spectra. Density measurements were carried out in water at 20 °C using a Digital Precision Density Meter DMA60/DMA602 (Anton Paar, Graz, Austria). From concentration series, in the range of  $2 \times 10^{-4}$  to  $4 \times 10^{-3}$  g/ml, the partial specific volume  $\bar{v}$  of the polymers was obtained [15] according to Eq. (1):

$$\rho = \rho_0 + (1 - \bar{v}\rho_0)c \quad (1)$$

Table 1  
Molecular characteristics of the PVBAC structures, trimethylammonium-A; dimethyl-*n*-butylammonium-B; pyridinium-C

Parameter	PVBAC-A		PVBAC-B		PVBAC-C	
$M_{\text{monomer}}$ (g/mol)	211.73		253.81		231.72	
Degree of polymerization	90	25	90	25	90	25
Degree of quaternization (%)	90	100	90	85	95	100
Contour length (nm)	22	6	22	6	22	6
Molecule volume <sup>a</sup> (nm <sup>3</sup> )	26.27	7.5	32.07	8.95	26.95	7.4
Molecule radius (nm)						
Sphere model	1.84	1.2	1.97	1.3	1.86	1.2
Rod model	0.60	0.62	0.68	0.68	0.62	0.62

<sup>a</sup> Calculated from the partial molar volumes in Table 4.

where  $\rho$  and  $\rho_0$  are the density of the solution and the solvent, respectively, and  $c$  designates the polymer concentration in g/cm<sup>3</sup>.

### 2.3. Column characterization

The ion-exchange capacity of the stationary phase has been determined by two independent techniques, atomic absorption spectrometry (AAS) [16] and a specific titration method [17].

#### 2.3.1. AAS

All columns were first equilibrated with 0.1 M NaCl for approximately 10 column volumes, followed by a front of 1.0 M (NH<sub>4</sub>)<sub>2</sub>SO<sub>4</sub>. The sodium content of the column effluent was analyzed by AAS (Model 1100A, Perkin-Elmer, Norwalk, CT, USA). Effluent fractions were diluted 1000 times in deionized water prior to the measurements. Na<sup>+</sup> standards (5, 10, 15, 20  $\mu$ M) served for calibration.

#### 2.3.2. Titration

The columns were equilibrated with 0.1 M HCl for approximately 10 column volumes, washed with 10 column volumes of deionized water and followed by a front of 1 M KNO<sub>3</sub>. The column effluent was collected and titrated against 0.01 M NaOH and phenolphthalein as an indicator. Table 2 summarizes the results for the ion capacity of both the material in Na and H form.

The stationary phase volume of the columns was determined by equilibrating with water at a flow rate of 0.1 ml/min and subsequent injection of 10  $\mu$ l of 1% NaNO<sub>3</sub>. In order to calculate the dead volume,  $V_0$ , of the column, the retention time for NaNO<sub>3</sub> with and without the column was recorded. Stationary phase volumes were calculated subtracting  $V_0$  from the total column volume (Table 2).

### 2.4. Adsorption isotherm measurements

Adsorption isotherms were measured as described elsewhere [18]. They monitor the stationary phase concentration (SPC) as a function of the mobile phase concentration (MPC). The chromatography system to record the breakthrough curves was assembled from a degasser (Merck, Switzerland), a HPLC pump (Merck–Hitachi L-7110, Switzerland), a Valco 10-port valve (Valco, VICI, Switzerland) and diode array detector (Hitachi L-7450, Switzerland). Five and two milliliters loops were employed for sample injection. A flow rate of 0.1 ml/min and a mobile phase of 0.075 and 0.225 M NaCl were used. The temperature of the columns was controlled to 25 °C (Oven L-7300 Hitachi, Switzerland). Two molar NaCl was used for column regeneration. Data collection and interpretation were carried out with Merck–Hitachi software. Adsorbed amounts were calculated using equation:

$$Q_{\text{ST}} = \frac{C_{\text{MP}}(V_{\text{B}} - V_0)}{V_{\text{ST}}} \quad (2)$$

Table 2  
Column parameters of sulfonated PS-DVB columns, MCX

	Column type			
	10/5	100/5	10/10	100/10
Pore size (nm)	10	100	10	100
Particle size ( $\mu$ m)	5	5	10	10
Column dimensions (mm)	2.1 $\times$ 125	2.1 $\times$ 125	4.6 $\times$ 30	4.6 $\times$ 30
Total column volume (ml)	0.4329	0.4329	0.4986	0.4986
Stationary phase volume (ml)	0.2529	0.1539	0.2386	0.1186
Ion capacity (mmol/ml SP)				
AAS (Na form)	2.62	2.62	2.51	6.86
Titration (H form)	1.92	1.75	2.12	4.54

where  $Q_{ST}$  is the amount of polymer adsorbed on the stationary phase,  $C_{MP}$  the concentration of the polymer in the mobile phase.  $V_B$ ,  $V_0$  and  $V_{ST}$  are the breakthrough volume of the substance, the dead volume of the column and the volume of the stationary phase. The variation of the polymer concentration was within the range of  $8 \times 10^{-4}$  to  $3 \times 10^{-2}$  monomol/l (0.2–8 mg/ml).

### 3. Results

#### 3.1. Adsorption isotherms

Various parameters are known to influence the adsorption behavior of charged macromolecules, polyelectrolytes, on oppositely charged surfaces [11]. Some of them have been selected and systematically varied in relevant ranges in order to identify their influence on the adsorption behavior on porous materials, such as represented by column materials. These included the contour length of the polyion, the hydrophobic character of the substituent at the quaternary ammonium group and the polymer concentration. Furthermore, the total ionic strength has been adjusted at different levels by addition of NaCl, intending to change the coil dimensions as well as the electrostatic interactions in solution. As indicated in Table 2, also the influence of the column material characteristics such as the pore size and the particle size were variables of interest for the adsorption experiments.

Figs. 2–6 illustrate, for selected experimental results, the tendencies of the adsorption behavior. Fig. 2 clearly reveals the influence of the chain length/molar mass of the molecules on the adsorbed amount on a 100 nm pore size column of 5  $\mu$ m particle size. Smaller molecules adsorb with higher amounts on this material but with differences concerning the substituents. The polyelectrolytes adsorb in the order  $A \gg B > C$ . Whereas for molecules with  $P_n = 90$  the adsorbed amounts do not exceed 2 mg/ml, the adsorbed amounts of the smaller molecules,  $P_n = 25$ , are remarkably higher,

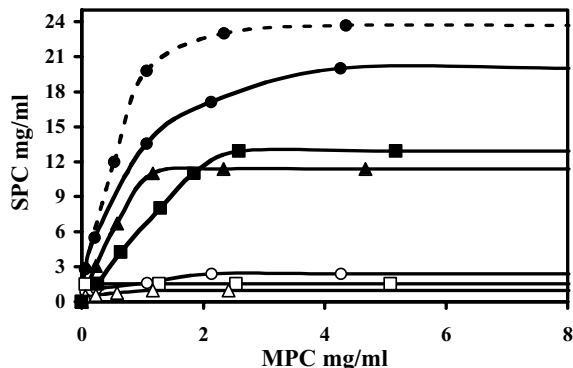


Fig. 2. Adsorption isotherms (stationary phase concentration, SPC, vs. mobile phase concentration, MPC) on MCX 100/5 in 0.075 M NaCl,  $P_n = 25$ : (●) PVBAC-A, (■) PVBAC-B, (▲) PVBAC-C;  $P_n = 90$ : (○) PVBAC-A, (□) PVBAC-B, (△) PVBAC-C; in 0.225 M NaCl,  $P_n = 25$  (---) PVBAC-A.  $T = 25^\circ\text{C}$ .

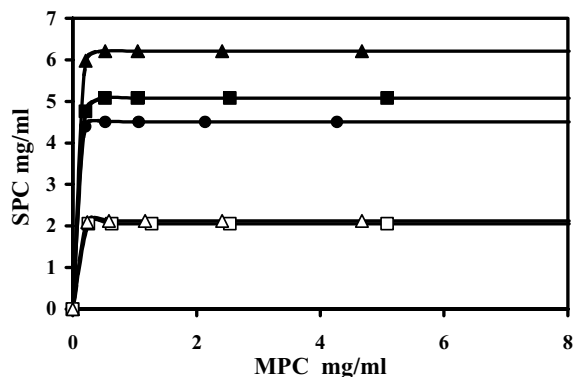


Fig. 3. Adsorption isotherms (stationary phase concentration, SPC, vs. mobile phase concentration, MPC) on MCX 100/10 in 0.075 M NaCl,  $P_n = 90$ : (□) PVBAC-B, (△) PVBAC-C; in 0.225 M NaCl: (●) PVBAC-A, (■) PVBAC-B, (▲) PVBAC-C.  $T = 25^\circ\text{C}$ .

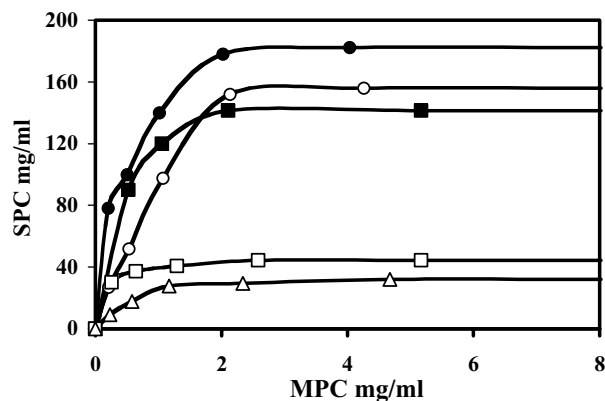


Fig. 4. Adsorption isotherms (stationary phase concentration, SPC, vs. mobile phase concentration, MPC) on MCX 100/10 in 0.075 M NaCl,  $P_n = 25$ : (○) PVBAC-A, (□) PVBAC-B, (△) PVBAC-C; in 0.225 M NaCl: (●) PVBAC-A, (■) PVBAC-B.  $T = 25^\circ\text{C}$ .

in the range of 11–20 mg/ml varying with the type of the substituent.

Similar adsorbed amounts have been obtained for the adsorption of the  $P_n = 90$  polymer series if a column of

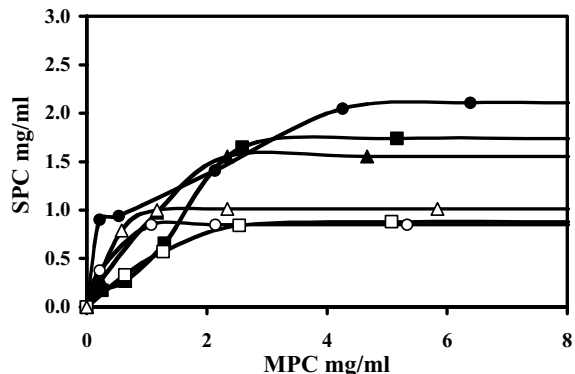


Fig. 5. Adsorption isotherms (stationary phase concentration, SPC, vs. mobile phase concentration, MPC) on MCX 10/10 in 0.075 M NaCl,  $P_n = 25$ : (●) PVBAC-A, (■) PVBAC-B, (▲) PVBAC-C;  $P_n = 90$ : (○) PVBAC-A, (□) PVBAC-B, (△) PVBAC-C.  $T = 25^\circ\text{C}$ .

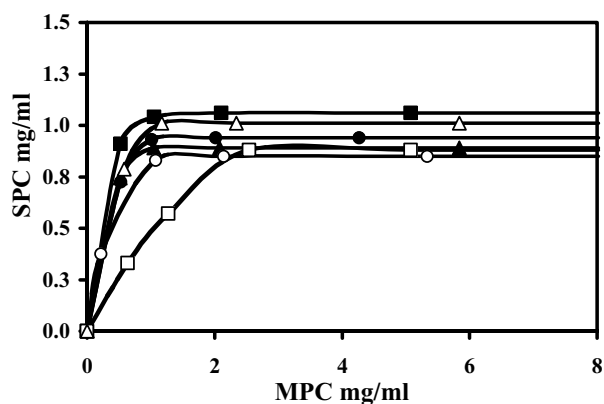


Fig. 6. Adsorption isotherms (stationary phase concentration, SPC, vs. mobile phase concentration, MPC) on MCX 10/10 in 0.075 M NaCl,  $P_n = 90$ : (○) PVBAC-A, (□) PVBAC-B, (△) PVBAC-C; in 0.225 M NaCl: (●) PVBAC-A, (■) PVBAC-B, (▲) PVBAC-C.  $T = 25^\circ\text{C}$ .

the same pore size but possessing 10  $\mu\text{m}$  particle size was employed. This is plotted in Fig. 3. However, the adsorbed amount increases approximately three-fold if the ionic strength increased performing the measurements in 0.225 M NaCl instead of 0.075 M NaCl. The order of adsorbed amount here is  $C > B > A$  in 0.225 M NaCl.

The investigation of the salt influence in the case of the  $P_n = 25$  series shows that the already high adsorbed amounts further increase (Fig. 4) employing the same column (100/10).

Concomitantly, at 0.075 M NaCl, a remarkable difference is visible for the adsorbed amounts of A and B with  $A \gg B$ . This was already evident on MCX 100/5 (compare the plots in Figs. 2 and 4). Increasing the salt concentration up to 0.225 M NaCl leads to a strong increase for B but a moderate one for A (Fig. 4). In total, the increase is approximately four-fold for B and approximately 20% for A. This agrees with the salt influence plotted in Fig. 2 for A where only an increase of approximately 20% is visualized, too.

Figs. 5 and 6 summarize the results for the lower pore size 10 nm and particle size of 10  $\mu\text{m}$  (MCX 10/10). Both molecule sizes adsorb on this material in a similar range with low amounts, less than approximately 2 mg/ml. Concerning the influence of the substituent the adsorbed amounts are slightly different. The initial slopes are not so steep, compared to the isotherms recorded for the pore size of 100 nm (Fig. 3). Adsorbing the  $P_n = 25$  and 90 polymer series on the 10/10 column in 0.075 M NaCl exhibits maximum adsorbed amounts in the range of 1.5–2 mg/ml ( $A > B > C$ ) and 0.9–1 mg/ml ( $A \approx B \approx C$ ), respectively (Fig. 5).

Increasing the salt concentration three times does not significantly increase the adsorbed amounts for  $P_n = 90$  (Fig. 6). All maximum values can be found in the range of 0.9–1.1 mg/ml, with somewhat steeper initial slopes for the higher salt concentration.

For the MCX 10/5 column very similar adsorbed amounts were obtained as shown for the MCX10/10 column in Figs. 5 and 6. Therefore, the data are not presented as graphs here.

Table 3

Influence of pore size, particle size, salt concentration and degree of polymerization,  $P_n$ , on the breakthrough time of PVBACs at saturation concentration

Column type <sup>a</sup>	Breakthrough time (min)			
	0.075 M NaCl		0.225 M NaCl	
	$P_n = 25$	$P_n = 90$	$P_n = 25$	$P_n = 90$
10/5	3.4–5.6	2.5–5	3–4	2.8–7
10/10	3.2–5	3–4	3.4–4.5	3–3.5
100/5	7–12	3–4.7	12	5–6
100/10	40–105	7–15	90–260	16–18

<sup>a</sup> Pore size (nm)/particle diameter ( $\mu\text{m}$ ).

### 3.2. Adsorption velocity

For technical processes as represented, for example, by protein displacement chromatography, the time scale at which a certain polymer acts as displacer is important. Therefore, also the breakthrough times of the investigated polymers in 0.075 and 0.225 M NaCl for both 10 and 100 nm pore size have been determined. For this purpose the mobile phase concentration at which the saturation polymer concentration appears has been selected. All data specified for the column type and the experimental conditions are summarized in Table 3.

They have been calculated directly from the chromatogram for the breakthrough at saturation concentration. The latest breakthrough occurs for the large pores, high salt concentration and lower molar mass of the polymer, in the range of 90–260 min. The time is relatively short for small pores, for both degrees of polymerization and salt concentrations (2.5–7 min). The increase of the salt concentration of the solution does not lead to any significant change in the breakthrough time in the case of 10 nm pores and also not for 100/5. In the case of MCX 100/10 the time increases by factor 2 only for shorter chains. The influence of the substituents has not been considered separately. It is included in the ranges presented in Table 3. No general trend was obvious.

### 3.3. Partial molar volumes

The partial molar volume, as a measure of the volume occupied by the molecules in solution, was calculated from the experimentally obtained partial specific volume by multiplying with the appropriate molar mass [15]. In addition, partial molar and specific volumes have been calculated applying the Durchschlag–Zipper (D–Z) procedure [19]. Table 4 summarizes all experimental and calculated values. The theoretical calculations consider the slight variation of the degree of quaternization. Nevertheless the resulting differences, less than 0.5%, are in the range of the experimental error. As expected, the experimental data do not reveal any molar mass influence. It has to be mentioned that the values include the

Table 4  
Experimental and calculated partial molar,  $\bar{V}$ , and partial specific volumes,  $\bar{v}$ , of PVBAc in water<sup>a</sup>

Structure	$P_n$	Experimental volumes		Calculated volumes		$\Delta\bar{V}$ (%)
		$\bar{V}_{\text{exp}}$ (cm <sup>3</sup> /monomol)	$\bar{v}_{\text{exp}}$ (cm <sup>3</sup> /g)	$\bar{V}_{\text{cal}}$ (cm <sup>3</sup> /monomol)	$\bar{v}_{\text{cal}}$ (cm <sup>3</sup> /g)	
A	90	175.7	0.830	180.4	0.852	2.7
	25	180.6	0.853	181.0	0.855	0.2
B	90	214.5	0.845	227.4	0.896	6.0
	25	215.5	0.849	226.4	0.892	5.1
C	90	180.3	0.778	183.8	0.793	1.9
	25	179.6	0.775	183.3	0.791	2.1

$$^a \Delta\bar{V} = (\bar{V}_{\text{cal}} - \bar{V}_{\text{exp}}) / \bar{V}_{\text{exp}} \times 100.$$

influence of interactions with the solvent, which is assumed to be strong for polyelectrolytes.

#### 4. Discussion

The experimental results clearly reveal the influence of the chain length, the type of the substituent at the quaternary ammonium group, the polymer concentration, and the ionic strength on the adsorption of cationic polyelectrolytes on negatively charged porous particles. Since no appropriate data have been reported yet, these initial studies have, to a certain extent, a screening character concerning the materials selection.

##### 4.1. Adsorbed amounts

In general, for porous particles as used in this study, the adsorption can occur on the surface of the spherical particles (outer surface) and inside the pores (inner surface). The adsorption on the outer surface should follow similar rules as described for the adsorption on flat surfaces [11]. Even for the 5  $\mu\text{m}$  particles the adsorption of the molecules investigated herein, possessing a maximum contour length of 22 nm (Table 1), can be considered as adsorption on a locally flat surface.

Adsorption only on the outer surface may be concluded from the data presented in Figs. 5 and 6 for the pore size 10 nm. Comparably low adsorbed amounts have been determined for both molecule sizes and ionic strengths. The slightly better adsorption for  $P_n = 25$  (Fig. 5) may result from less sterical hindrance for the smaller polymer molecules when they arrange themselves on the surface. A denser package of the smaller molecules is probably achieved. Though with maximum values of 2 mg/ml the SPC is quite low. The situation does not change significantly if the salt concentration increases. However, the saturation already occurs at lower mobile phase concentrations implying advanced arrangement. From the experiments with 10 nm pore size, adsorbed amounts up to 2 mg/ml may be concluded as complete pore exclusion for both particle sizes.

A different situation exists for the particles with 100 nm pore size. There, a molar mass/molecule size effect is clearly evident.  $P_n = 25$  molecules adsorb with significantly higher amounts than the  $P_n = 90$  molecules. Moreover, the substituent effect is much more pronounced. In detail, the differences caused by the substituent type were estimated as less than 1.5 mg/ml if the adsorption occurred only on the outer surface. These differences were up to 10 mg/ml for MCX 100/5 and even approximately 110 mg/ml for MCX 100/10. In general, the trimethyl substituted compound PVBAc-A adsorbed with the highest amounts. Only in the case of  $P_n = 90$ , but not for  $P_n = 25$ , an inverse adsorption behavior was detected at high added salt amount but with a total difference of only 1.5 mg/ml. This tendency was found for other experiments not reported here but needs further investigation. With increasing hydrophobicity, the solubility in aqueous solution decreases leading to more compact molecule coils in solution. This effect is supported by the addition of salt. Moreover, at the same polyelectrolyte concentration, the effect of added salt is stronger on longer polyion chains than on shorter ones [20].

The total adsorbed amounts imply the diffusion into pores of 100 nm for all  $P_n = 25$  molecule types, independent of their chemical structure. Furthermore, the experimental results indicate differences for 100/5 and 100/10. These findings are evident comparing Figs. 2 and 4. Whereas for the column 100/5 only 4.3% of surface charges are complexed by PVBAc-A, this percentage is increased to 12.4% for 100/10. The latter possess a higher ion capacity (Table 2). However, it is not clear if the higher ion capacity results from a higher surface charge density or a different ratio of the surface area to the stationary phase volume for these two columns. A higher surface charge density could attract the molecules more strongly though more molecules can adapt to a larger surface.

The salt concentration can have various effects on the solution behavior of polyelectrolytes and, consequently, on the structure of the adsorbed layer [11]. Increasing the ionic strength by adding salt reduces the Debye length and forces conformational changes. The molecular dimensions decrease and the intermolecular repulsion is reduced. This yields higher adsorbed amounts (Figs. 2–4). The salt

Table 5  
Debye length,  $l_D$ , the ratio of the Debye length to the contour length,  $l_D/L$ , and the overlap concentration,  $c^*$ , of PVBAC molecules

$P_n$	$l_D$ (nm)		$l_D/L$		$c^*$ (monomol/l)
	0.075 M NaCl	0.225 M NaCl	0.075 M NaCl	0.225 M NaCl	
90	11	6	0.5	0.27	$1.3 \times 10^{-2}$
25	11	6	1.8	1	$1.8 \times 10^{-2}$

concentration can have a different effect in regard to the chemical structure. As presented in Fig. 4 it causes a strong increase of the adsorbed amount for PVBAC-B, the more hydrophobic molecule, but a comparably moderate one for PVBAC-A (see also Fig. 2). With 44 mg/ml (PVBAC-B) and 32 mg/ml (PVBAC-C) the two molecules are in the same range at 0.075 M NaCl but much lower than PVBAC-A. The increased ionic strength at 0.225 M NaCl seems to affect the solution properties of the molecules possessing more voluminous and/or hydrophobic substituents (B and C) stronger than those of the PVBAC-A structure. On the other hand, it can also be concluded that the PVBAC-A already enters the pores at 0.075 M NaCl resulting in an almost saturation of the inner surface.

A slight effect of the ionic strength is observed for  $P_n = 90$  on MCX 100/10 with the inversion of the substituent influence already discussed above. The comparison of data in Figs. 3 and 6 suggests minor pore occupation.

#### 4.2. Molecular dimensions

The previous discussion did not separate the two superimposing effects size/steric exclusion and electrostatic exclusion. For polyelectrolytes both processes are affected by the concentration and the ionic strength of the solution, which modify the molecule dimensions and the electrostatic interactions in solution. Furthermore, also the range of the electrostatic atmosphere of the surface is influenced. The Debye length,  $l_D$ , serves as a measure for the ionic atmosphere though it has to be noted that it is strictly valid only for point-like charges. The calculated Debye lengths summarized in Table 5 consider both the ions present from the polyelectrolyte molecules and the added salt [15,20,21]. Since the salt concentration exceeds the experimental polyelectrolyte concentrations it is obvious that the salt concentration dominates the total ionic strength and, therefore, the Debye length. (The independence of the degree of polymerization results from reference to one monomer unit, for the polyelectrolyte concentration expressed in monomol/l.) Comparing the data of Tables 1 and 5 it is evident that  $l_D$  exceeds the molecule radius and, therefore, electrostatic interaction can be suggested in this length scale. Furthermore, it is obvious from the electrostatic dimensions that no molecule should enter pores of 10 nm what is in agreement with the experimental results.

The majority of the adsorption experiments have been performed below the critical overlap concentration [20] where the single molecules are separated in solution and start to

expand. The appropriate concentrations calculated for aqueous solutions without the addition of salt are given in Table 5. If salt is added these concentrations become higher. If, in addition, the Debye length equals or exceeds the contour length, as it is the case for  $P_n = 25$ , the counterion activity increases as the result of the extended ionic atmosphere. Nevertheless, even the full extension of the  $P_n = 90$  molecules cannot explain the exclusion from 100 nm pores. Therefore, it can be concluded that strong long-range electrostatic effects are the reason for the pore exclusion on MCX 100 nm. As it is known from the process of polyelectrolyte multilayer formation on flat oppositely charged surfaces, only partial charge neutralization of the polyelectrolyte occurs during the adsorption process if a certain chain length is exceeded [22]. The remaining excess charges (loops, tails) act repulsive to the incoming equally charged polyelectrolyte molecules and may prevent further pore entering, in particular, if the polyelectrolyte molecules adsorb first at the outer surface and around the pore entrance. This repulsion may also cause a limited package density. In addition, overlapping of the ionic atmospheres at the low ionic strengths should be discussed [23,24].

#### 4.3. Ion capacity

The comparison of the ion capacity of the columns indicated in Table 2 with the experimentally determined maximum adsorbed amounts reveals that only a low portion of the surface charges is complexed by the polyions. One milligram of polymer corresponds to  $4.7 \times 10^{-3}$ ,  $3.9 \times 10^{-3}$ ,  $4.3 \times 10^{-3}$  mol monomer units for PVBAC-A, -B, and -C, respectively. For the adsorption on the outer surface, pore exclusion, only approximately 0.06–0.3% of the binding sites are neutralized by the polyions. In the case of adsorption inside the pores this percentage increases up to 12.4% for PVBAC-A on MCX 100/10 or 4.3% on MCX 100/5 if the values from AAS are considered (compare the discussion in Section 4.1). Although the ion capacities obtained from the two analytical methods applied differ, the tendency, conclusions, and orders of magnitude remain valid.

#### 4.4. Adsorption process

In addition to the static parameters of the discussion above, the duration of the adsorption process under specific conditions also have to be considered. It was demonstrated that the adsorbed amounts on a defined stationary phase volume might increase significantly if material possessing

larger pores is employed. However, one has to consider the increased breakthrough time, which is assumed to correlate with the displacement time. Insufficient displacement may cause low yields and/or displacer breakthrough before the molecules of interest are displaced.

#### 4.5. General remarks

Evaluating the reliability of the experimental results it has to be noted that special attention is necessary with regard to column regeneration, in particular, in the case of porous particles. The application of larger particles avoids increasing backpressure.

### 5. Conclusions and outlook

The separation and purification of biomolecules by ion-exchange displacement chromatography require experimental conditions, with regard to pH and salt concentration, for which strong electrostatic interactions can be expected. This has to be considered for the process development and optimization. At present such interactions, including the effects of molecule size, chemical structure as well as process conditions, cannot be predicted quantitatively on the basis of molecular approaches.

Therefore, empirically derived models and/or relationships based on reliable experimental data and subsequent comparison with theoretical calculations, as performed in this study, may serve to overcome this gap. As it is evident from the influences identified herein, such studies only succeed if well-defined molecules and materials are used.

More experiments with molecules possessing chain lengths between the two of this study, as well as the variation of the ionic strength, will contribute to further quantification of the interrelation between size exclusion and electrostatic exclusion. The time scale of the adsorption process has to be considered for practical applications. Finally, the knowledge gained from the adsorption studies on porous particles may also be of interest for surface and materials modification. Moreover, it may contribute to overcome existing difficulties if polyelectrolytes are characterized by size exclusion chromatography with the conclusion that size exclusion not only occurs with regards to the hydrodynamic radius but is additionally influenced by electrostatic dimensions.

### Acknowledgements

We thank W. Jaeger, Fraunhofer Institute of Applied Polymer Research, Golm, Germany, for supporting the polymer synthesis. The Swiss National Science Foundation is acknowledged for financial support (grant 2100-611314).

### References

- [1] R. Freitag, in: H.Y. Aboul-Enein (Ed.), *Analytical and Preparative Separation Methods for Biomolecules*, Marcel Dekker, New York, 1999.
- [2] A.A. Shukla, R.R. Deshmukh, J.A. Moore, S.M. Cramer, *Biotechnol. Progr.* 16 (2000) 1064.
- [3] V. Natarajan, S. Ghose, S.M. Cramer, *Biotechnol. Bioeng.* 78 (2000) 365.
- [4] R. Freitag, C. Wandrey, in: R. Freitag (Ed.), *Biotechnology Intelligence Unit 4*, Landes Bioscience, Georgetown, TX, 2003.
- [5] C. Wandrey, R. Freitag, *Polym. News* 25 (2000) 554.
- [6] C.C. Tugcan, S.K. Park, J.A. Moore, S. Cramer, *Ind. Eng. Chem. Res.* 41 (2002) 6482.
- [7] B. Schmidt, C. Wandrey, R. Freitag, *J. Chromatogr. A* 944 (2002) 149.
- [8] A. Kumar, I.Y. Galaev, B. Mattiasson, *J. Chromatogr. B* 741 (2000) 103.
- [9] V. Natarajan, S.M. Cramer, *J. Chromatogr. A* 876 (2000) 63.
- [10] C.A. Brooks, S.M. Cramer, *AIChE J.* 38 (1992) 1969.
- [11] G.J. Fleer, M.A. Cohen Stuart, J. Scheutjens, T. Cosgrove, B. Vincent, *Polymers at Interfaces*, Chapman & Hall, London, 1993.
- [12] C. Wandrey, D. Hunkeler, U. Wendler, W. Jaeger, *Macromolecules* 33 (2000) 7136.
- [13] U. Wendler, J. Bohrisch, W. Jaeger, G. Rother, H. Dautzenberg, *Macromol. Rapid Commun.* 19 (1998) 185.
- [14] W. Jaeger, U. Wendler, A. Lieske, J. Bohrisch, C. Wandrey, *Macromol. Symp.* 161 (2000) 87.
- [15] C. Wandrey, A. Bartkowiak, D. Hunkeler, *Langmuir* 15 (1999) 4062.
- [16] S.D. Gadam, G. Jayaraman, S.M. Cramer, *J. Chromatogr.* 630 (1993) 37.
- [17] A.A. Shukla, S.S. Bae, J.A. Moore, S.M. Cramer, *J. Chromatogr. A* 827 (1998) 295.
- [18] J. Jacobson, J. Frenz, J. Horvath, *J. Chromatogr.* 316 (1984) 53.
- [19] H. Durchschlag, P. Zipper, *Prog. Colloid Polym. Sci.* 94 (1994) 20.
- [20] C. Wandrey, *Langmuir* 15 (1999) 4069.
- [21] H. Dautzenberg, W. Jaeger, J. Kötzt, B. Philipp, C. Seidel, D. Stscherbina, *Polyelectrolytes: Formation, Characterization and Application*, Hanser, Munich, 1994.
- [22] G. Decher, in: G. Decher, J.B. Schlenoff (Eds.), *Multilayer Thin Films*, Wiley-VCH, Weinheim, 2003.
- [23] M. Antonietti, A. Briel, S. Förster, *J. Chem. Phys.* 105 (1996) 7795.
- [24] M. Antonietti, A. Briel, F. Gröhn, *Macromolecules* 33 (2000) 5950.